

MEASURED EFFECTS OF FREQUENCY DIVISION
ON THE PERFORMANCE OF PULSE COUNTING
FREQUENCY DEMODULATORS

Duong Tuan Viet

INTERNATIONAL
DISTRIBUTED REPORT

DUDLEY KNOX LIBRARY
NAVAL POSTGRADUATE SCHOOL
MONTEREY, CALIF. 93940

INTERNALLY DISTRIBUTED

REPORT
NAVAL POSTGRADUATE SCHOOL
Monterey, California



THESIS

MEASURED EFFECTS OF FREQUENCY DIVISION
ON THE PERFORMANCE OF PULSE COUNTING
FREQUENCY DEMODULATORS

by

Duong Tuan Viet

June 1976

Thesis Advisor:

Glen A. Myers

Approved for public release; distribution unlimited.

T174972

REPORT DOCUMENTATION PAGE		READ INSTRUCTIONS BEFORE COMPLETING FORM
1. REPORT NUMBER	2. GOVT ACCESSION NO.	3. RECIPIENT'S CATALOG NUMBER
4. TITLE (and Subtitle) Measured Effects of Frequency Division on the Performance of Pulse Counting Frequency Demodulators		5. TYPE OF REPORT & PERIOD COVERED Master's Thesis; June 1976
7. AUTHOR(s) Duong Tuan Viet		6. PERFORMING ORG. REPORT NUMBER
9. PERFORMING ORGANIZATION NAME AND ADDRESS Naval Postgraduate School Monterey, California 93940		8. CONTRACT OR GRANT NUMBER(s)
11. CONTROLLING OFFICE NAME AND ADDRESS Naval Postgraduate School Monterey, California 93940		10. PROGRAM ELEMENT, PROJECT, TASK AREA & WORK UNIT NUMBERS
14. MONITORING AGENCY NAME & ADDRESS (if different from Controlling Office) Naval Postgraduate School Monterey, California 93940		12. REPORT DATE June 1976
		13. NUMBER OF PAGES 40
		15. SECURITY CLASS. (of this report) Unclassified
16. DISTRIBUTION STATEMENT (of this Report) Approved for public release; distribution unlimited.		15a. DECLASSIFICATION/DOWNGRADING SCHEDULE
17. DISTRIBUTION STATEMENT (of the abstract entered in Block 20, if different from Report)		
18. SUPPLEMENTARY NOTES		
19. KEY WORDS (Continue on reverse side if necessary and identify by block number) Frequency Division in FM System		
20. ABSTRACT (Continue on reverse side if necessary and identify by block number) The measured performance of frequency demodulators that use frequency division before demodulation is presented. Digital data (square wave modulating signal) is used in the experiment. This binary signal permits a quantitative measure of performance, namely probability of error in recovering the data. Noise is added to a carrier that is frequency modulated by the square wave data. The recovered waveform at the demodulator output is compared with		

Unclassified

SECURITY CLASSIFICATION OF THIS PAGE(When Data Entered)

the original data and errors are counted. The results are presented as a plot of probability of error vs ratio in decibels of signal power to noise power. Results for frequency division by factors of 1,2,6, 8 and 12 are given.

From the experimental results, it is concluded there is no significant improvement in system performance with frequency division.

Unclassified

SECURITY CLASSIFICATION OF THIS PAGE(When Data Entered)

Measured Effects of Frequency Division
on the Performance of Pulse Counting Frequency Demodulators

by

Duong Tuan Viet
B. S. Vietnamese Military Academy, 1970
B.S.E.E. Naval Postgraduate School, 1975

Submitted in partial fulfillment of the
requirements for the degree of

MASTER OF SCIENCE IN ELECTRICAL ENGINEERING

from the
NAVAL POSTGRADUATE SCHOOL

ABSTRACT

The measured performance of frequency demodulators that use frequency division before demodulation is presented. Digital data (square wave modulating signal) is used in the experiment. This binary signal permits a quantitative measure of performance, namely probability of error in recovering the data.

Noise is added to a carrier that is frequency modulated by the square wave data. The recovered waveform at the demodulator output is compared with the original data and errors are counted. The results are presented as a plot of probability of error vs ratio in decibels of signal power to noise power. Results for frequency division by factors of 1,2,6,8 and 12 are given.

From the experimental results, it is concluded there is no significant improvement in system performance with frequency division.

TABLE OF CONTENTS

I.	INTRODUCTION	8
II.	SUMMARY OF REPORT	10
III.	EXPERIMENTAL SYSTEM	13
IV.	PROCEDURE AND CONCLUSION	17
	APPENDIX A. Schematic Diagrams	27
	LIST OF REFERENCES	39
	INITIAL DISTRIBUTION LIST	40

LIST OF FIGURES

1.	Probability P_e of Error vs SNR	11
2.	Block Diagram of Experimental System	12
3.	Waveforms Appearing in the Experimental System with No Noise	14,15 & 16
4.	Amplitude vs Frequency Response Characteristic	18
5.	Spectrum of FM Signal at Output of Hard Limiter ($f_c = 455$ kHz)	20
6.	Spectrum of FM Signal at Output of the Frequency Divider ($N = 2$)	21
7.	Spectrum of FM Signal at Output of the Frequency Divider ($N = 6$)	22
8.	Spectrum of FM Signal at Output of the Frequency Divider ($N = 8$)	23
9.	Spectrum of FM Signal at Output of the Frequency Divider ($N = 12$)	24
A-1.	Error Measurement Gating Circuit	28
A-2.	Summing Amplifier	29
A-3.	Hard Limiter	31
A-4.	Circuit of Frequency Dividers	32
A-5.	Pulse Counting Demodulator	33
A-6.	Frequency Response of Lowpass Filter when Cut-off Frequency f_u is 1, 4 and 6 kHz	34
A-7.	Error Detection Circuit	35
A-8.	Error Decision Circuit	37
A-9.	Waveforms Associated with Error Circuits	38

LIST OF SYMBOLS

b	Bandwidth of modulating signal
$d(t)$	Modulating signal (square wave)
$\hat{d}(t)$	Replica of $d(t)$
f_c	Center frequency of FM signal (carrier frequency)
f_m	Frequency of modulating signal
f_u	Upper cut-off frequency of lowpass filter
k_ω	Property of modulator (constant)
$m(t)$	Modulating signal (any waveform)
$n(t)$	Noise voltage at output of mechanical bandpass filter
$p(t)$	Output of pulse generator
$v_c(t)$	Frequency modulated carrier signal
$v_d(t)$	Output of monostable multivibrator
$v_i(t)$	Output of square wave generator
$v_s(t)$	Output of summing amplifier
$v_L(t)$	Output of hard limiter
$v_N(t)$	Output of divide by N circuit
$v_T(t)$	Output of error measurement gating circuit
A	Amplitude of FM signal
B	Bandwidth of FM signal
N	Frequency division factor
N_p	Noise power
S	Signal power
β	Modulation index
Δf	Frequency deviation of the carrier
ω	Radian frequency
$\rho(t)$	Phase modulation

I. INTRODUCTION

This report details the findings of an experimental investigation of the use of frequency dividers in the demodulation of frequency modulated (FM) carrier signals.

A sinusoidal signal when frequency modulated by a message $m(t)$ or data is described by the equation [Ref. 1]

$$v_c(t) = A \cos [\omega_c t + k_\omega \int m(t) dt].$$

where the amplitude A is constant, $f_c = \frac{\omega_c}{2\pi}$ is the carrier frequency in Hertz, the constant k_ω is a property of the modulator, and t is ordinary time. This equation can be written also as

$$v_c(t) = A \cos [\omega_c t + \beta \rho(t)]$$

where the maximum value of $\rho(t)$ is 1 and where β is then the peak phase deviation of the carrier or modulation index.

The constant β is important in FM because it is a measure of the bandwidth of $v_c(t)$. A rule of thumb is that the radio frequency bandwidth B of the FM signal is:

$$B = 2(\beta + b)$$

where b is the bandwidth of the modulating signal $m(t)$ [Ref. 1]. The bandwidth B can be increased, then, by increasing β in the transmitter, and this is often done (wideband FM).

A common method of increasing β is through use of frequency multipliers which consist of devices which create harmonics of the FM signal. Factors of 2 and 3 are easily obtained using class C amplifiers, for example. Series connection of these devices and/or other devices provide

larger integer multipliers. A times M frequency multiplier increases β by a factor of M . In some applications, M may be as large as a few hundred.

In the receiver, the now wideband FM signal is demodulated directly using conventional methods (phase-locked loops, Foster-Seeley discriminator, ratio detector, pulse counting discriminator). Typically, no attempt is made to alter β before demodulation.

In this work, we investigate the performance of a pulse counting discriminator as β is changed (decreased). Frequency dividers which are available in integrated circuit form can be used to decrease β in the same way frequency multipliers are used to increase β . In this work, division by factors of 2,4,6,8 and 12 are instrumented.

A square wave is used as a modulating signal (message). This is chosen for convenience and also to permit a quantitative measure (probability of error) of system performance. The use of this periodic digital signal for the data also provides line spectra which can be readily related to theory.

Noise is added to the system to determine performance as the ratio of signal power to noise (SNR) varies. The results are documented for various values of division factor N .

II. SUMMARY OF REPORT

The results of this experimental work are presented in Figure 1 which shows the probability of error occurring in the transmission of binary digital data (square wave) through the system as a function of the ratio in decibels of signal power to noise power at the input to the demodulation portion of the receiving system. The results are shown for frequency division by $N = 2, 4, 6, 8, 12$. The result for no division ($N=1$) is also presented, and this data agrees well with the theory (dashed curve) [Ref. 2].

From this data we conclude there is no significant improvement in system performance with frequency division. There is a possible reduction in noise power with frequency division because of reduced signal bandwidth. However, frequency division also reduces the amplitude of the recovered signal (usable demodulator output). The result is no net improvement in system performance.

Section III of this report treats the experimental system used in this study and presents typical waveforms associated with the system. In Section IV, the experimental procedure is detailed along with reasons for choice of system parameters. Conclusions on procedure and results are presented in Section IV. The Appendix provides detail on instruments and circuits used to realize the system described in the next Section.

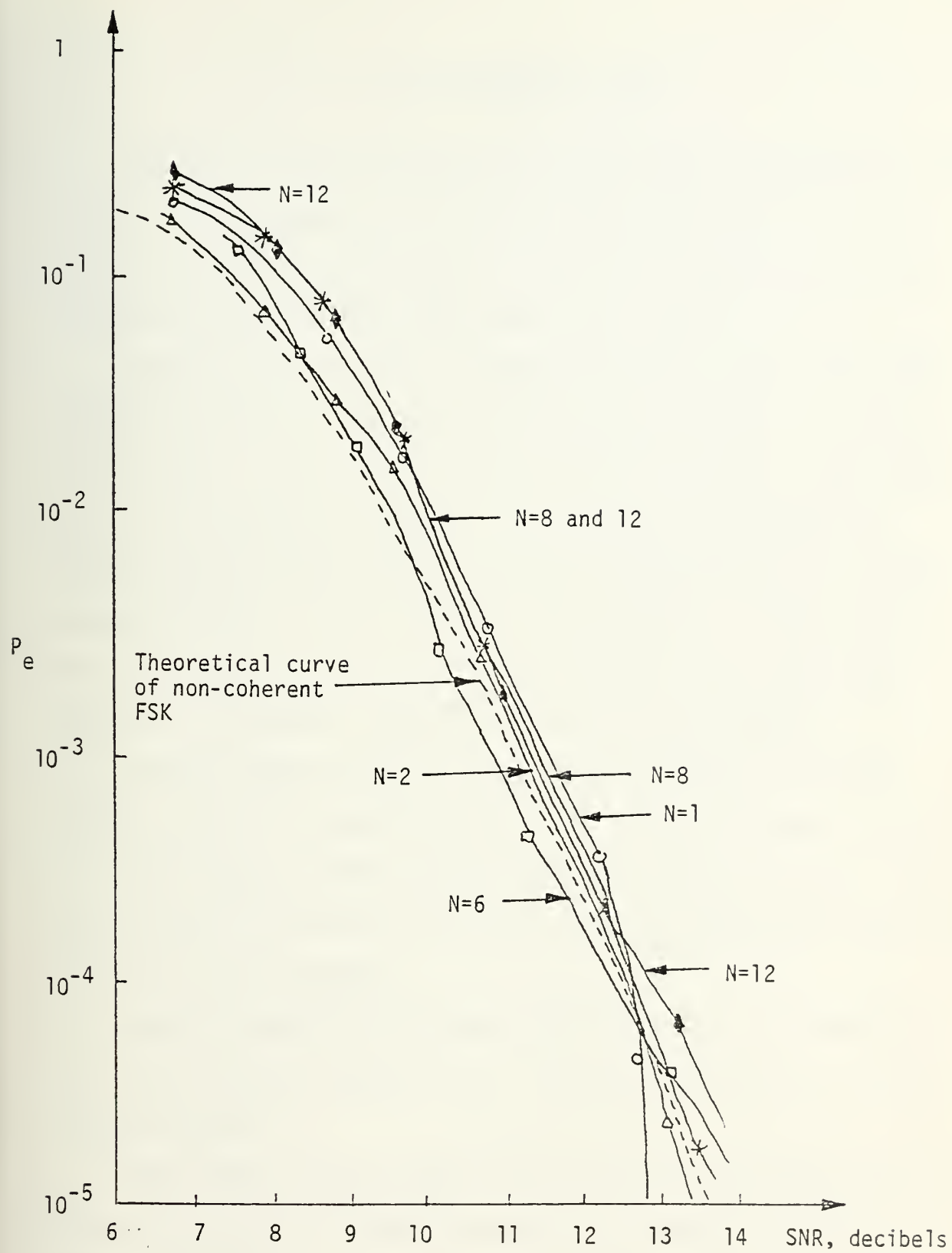


FIGURE 1. PROBABILITY P_e OF ERROR VS SNR

III. EXPERIMENTAL SYSTEM

Figure 2 is a block diagram of the experimental system used in this study. Detailed description of the operation and realization of each block is contained in the Appendix. Figure 3 indicates typical waveforms associated with the system when noise is absent.

The data source provides a square wave (binary) signal $d(t)$ which frequency modulates a sinusoidal carrier of frequency equal to 455 kHz to form $v_c(t)$. Noise $n(t)$ filtered to lie in a passband of width equal to 10 kHz about 455 kHz is added to the FM signal. Measurement of signal power and signal plus noise power are made at the output of the summing amplifier using a true RMS reading voltmeter. These readings are used to obtain signal-to-noise ratio (SNR) of the voltage $v_s(t)$ applied to the receiver (demodulator) portion of the system.

The hard limiter removes the amplitude variations of the input signal $v_s(t)$ while preserving the frequency variations (zero crossings).

The frequency divider reduces the number of transitions per second of $v_L(t)$ (output of the hard limiter) by a factor of $\frac{1}{N}$ as seen by comparing $v_N(t)$ and $v_L(t)$ in Figure 3.

The pulse counting discriminator (PCD) consists of a monostable multivibrator and a lowpass filter. The PCD output $\hat{d}(t)$ is a replica of the data $d(t)$.

Measurement circuits compare $d(t)$ and $\hat{d}(t)$ to count errors and data rate from which error probability can be calculated and associated with SNR.

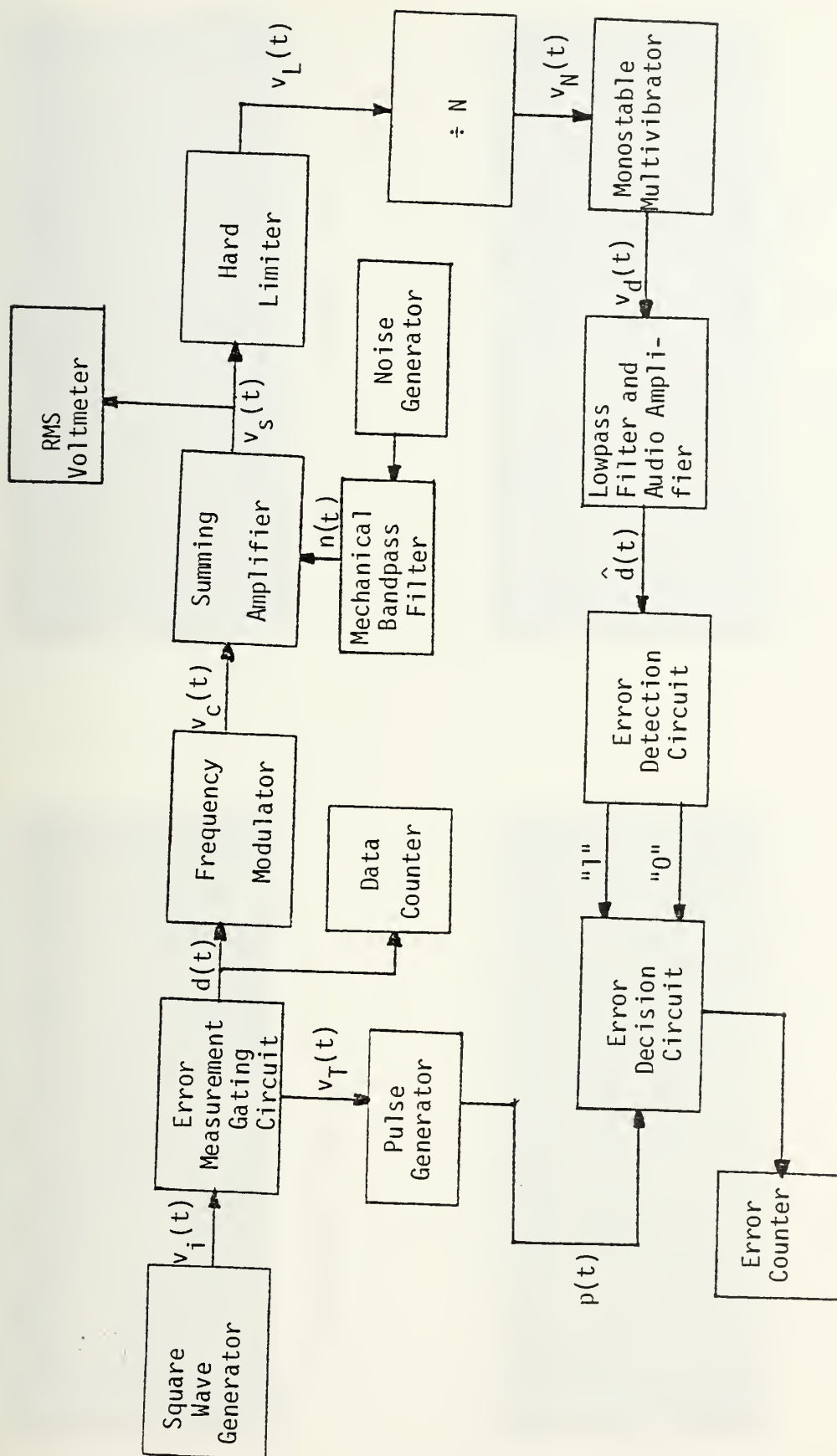
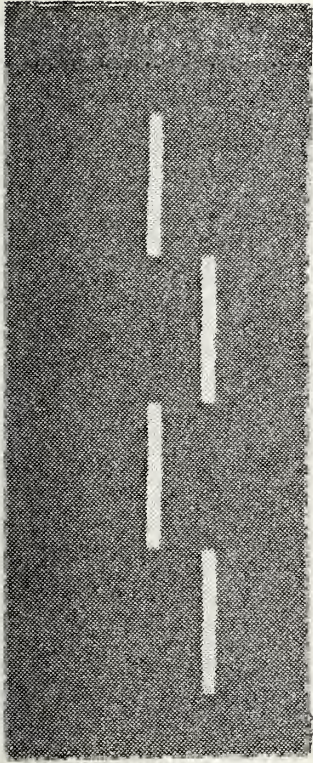
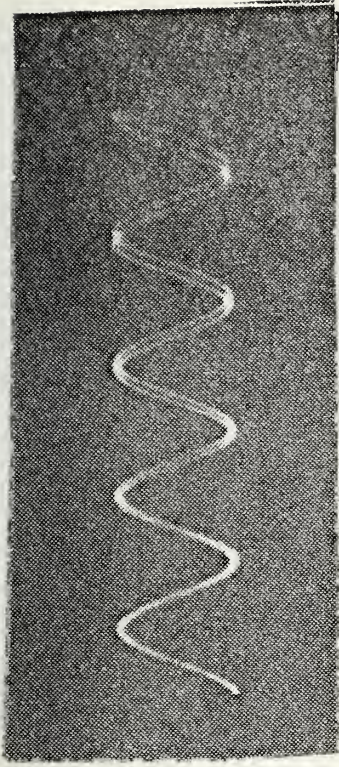


Figure 2. BLOCK DIAGRAM OF EXPERIMENTAL SYSTEM



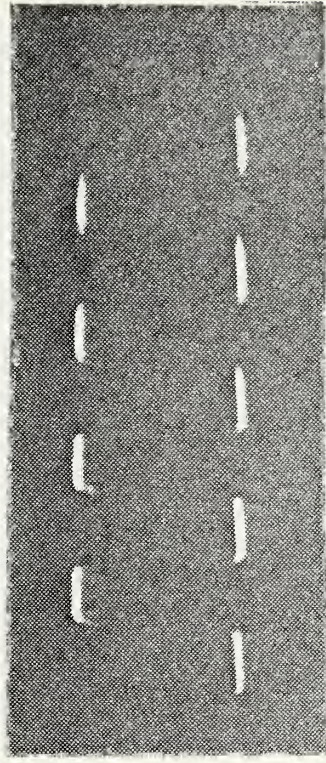
(a) Modulating signal $d(t)$



(b) Input $v_c(t)$ of summing amplifier

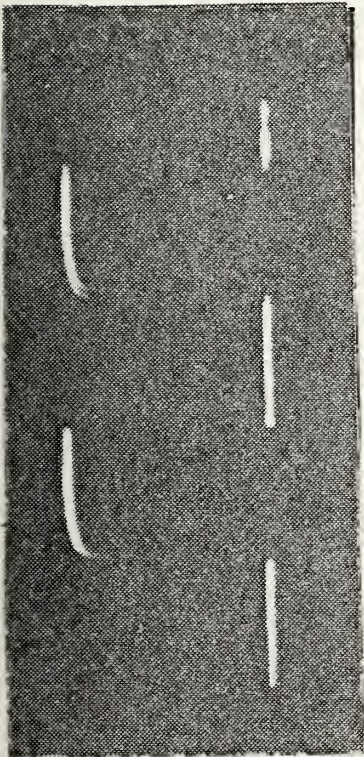


(c) Output $v_s(t)$ of summing amplifier

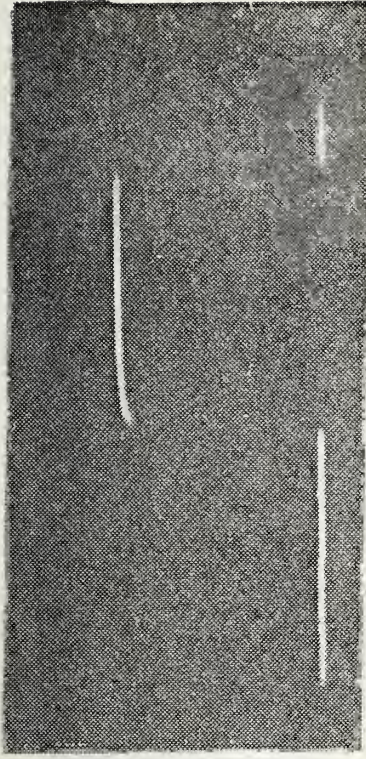


(d) Output $v_L(t)$ of hard limiter

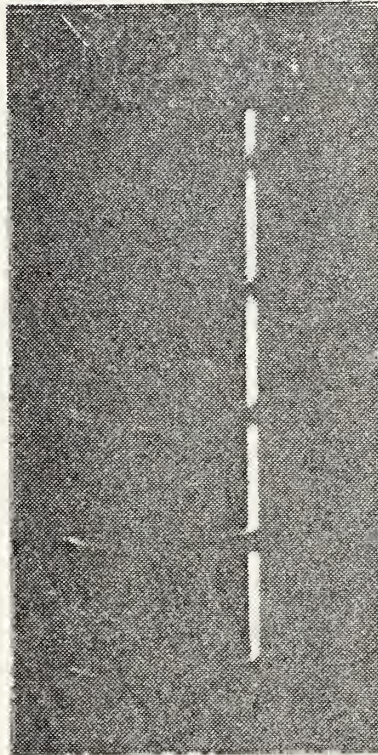
Figure 3. WAVEFORMS APPEARING IN THE EXPERIMENTAL SYSTEM WITH NO NOISE



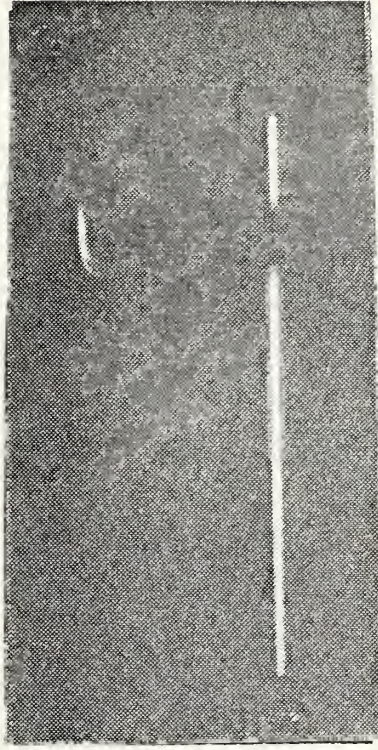
(e) Output $v_N(t)$ of divide by 2 circuit



(f) Output $v_N(t)$ of divide by 4 circuit

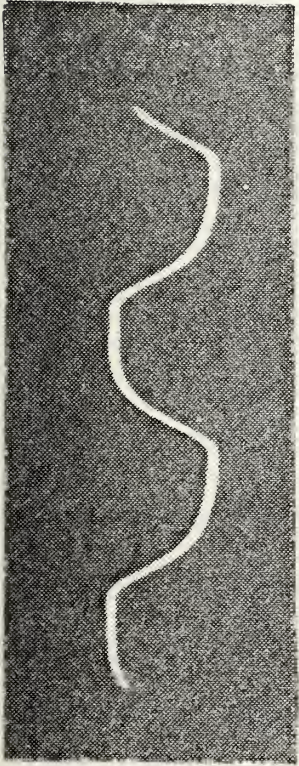


(g) Typical output $v_d(t)$ of monostable multivibrator (pulse width = 500 ns)

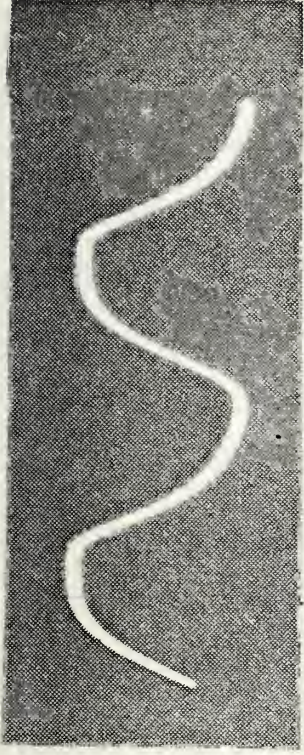


(h) Typical output $v_d(t)$ of monostable multivibrator (pulse width = 3 μ s)

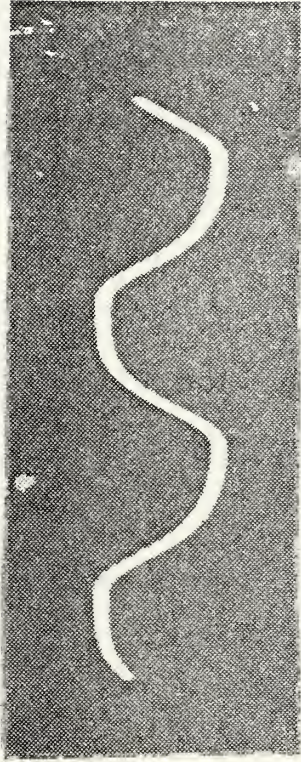
FIGURE 3. WAVEFORMS APPEARING IN THE EXPERIMENTAL SYSTEM WITH NO NOISE



(k) Recovered signal $\hat{d}(t)$ without frequency division ($N = 1$)



(l) Recovered signal $\hat{d}(t)$ when $N = 6$



(m) Recovered signal $\hat{d}(t)$ when $N = 12$

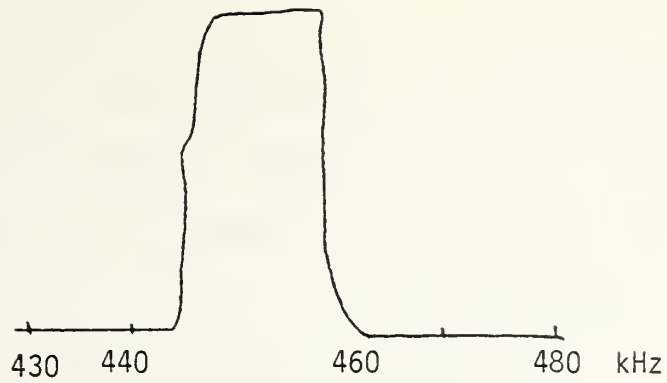
FIGURE 3. WAVEFORMS APPEARING IN THE EXPERIMENTAL SYSTEM WITH NO NOISE

IV. PROCEDURE AND CONCLUSION

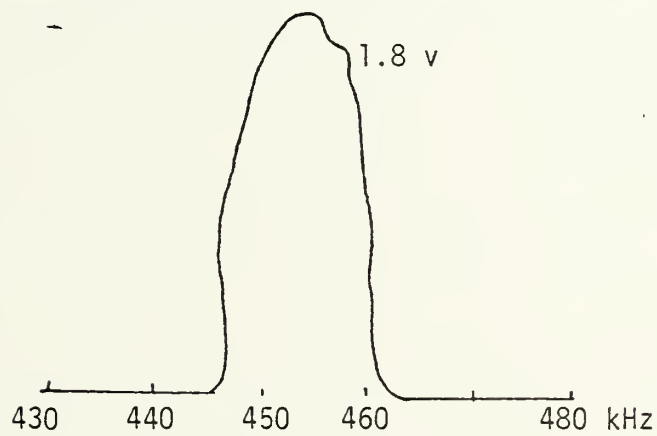
In a typical superheterodyne radio receiving system, the input voltage is bandlimited by the intermediate-frequency (IF) amplifier before demodulation. The system used here (Figure 2) filters noise only. This is done because of the characteristics of the bandpass filter (BPF) available. The mechanical filter having the amplitude response shown in Figure 4(a) is used. Manufacturer's data on the filter indicates a nonlinear phase vs frequency characteristic near the edges of the passband. This nonlinearity is severe enough to cause considerable distortion of a FM signal applied to the filter. For that reason, it was decided to filter only the noise. To relate the test results to a practical radio receiver, it is then necessary to adjust the period and amplitude of the data $d(t)$ of Figure 3 such that the significant sidebands of $v_c(t)$ remain within the 13 kHz passband of the mechanical filter.

The amplitude vs frequency response (in the vicinity of 455 kHz) of the mechanical BPF and summing amplifier combined is shown in Figure 4(b) and that of the mechanical BPF, summing amplifier, and hard limiter combined is shown in Figure 4(c).

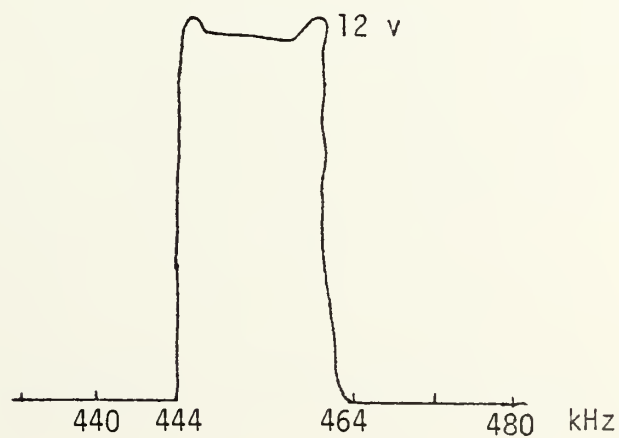
In the experiment, the frequency (data rate) of the square wave modulating signal is set at 1 kHz. Figure 5 clearly shows the line spectrum of the FM carrier and the lines spacing of 1 kHz. Figure 6 is the line spectrum of the FM signal after frequency division by 2. Note that the center carrier frequency is now $455 \text{ kHz} / 2 = 227.5 \text{ kHz}$ as expected. Further, there are fewer lines in this spectrum relative to that of Figure 5 which indicates the modulation index after division is



(a) Mechanical filter; Bandwidth = 13 kHz,
center frequency = 455 kHz.



(b) Mechanical filter and summing amplifier.

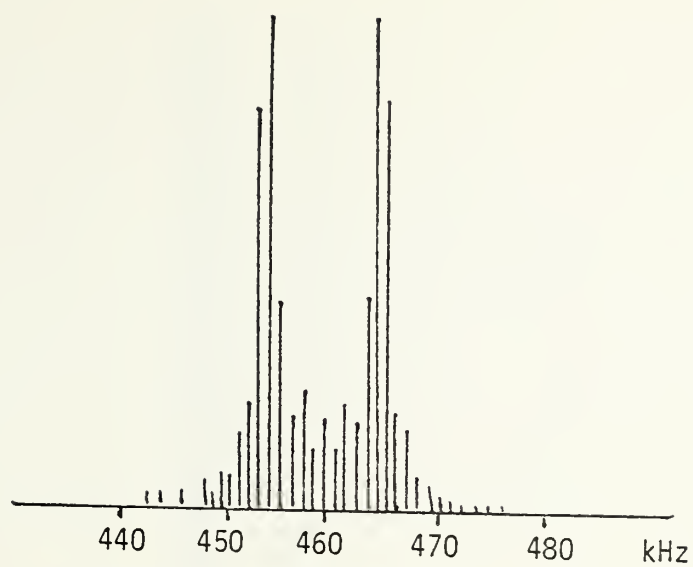


(c) Mechanical filter, summing amplifier,
and hard limiter.

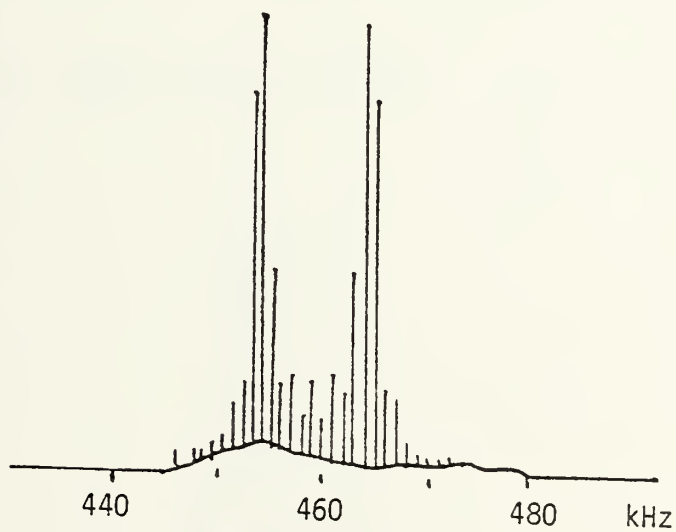
Figure 4. AMPLITUDE VS FREQUENCY RESPONSE CHARACTERISTICS

less than (equals one-half) that of the input FM signal. However, the line spacing of 1 kHz is preserved, again as expected.

Similar reasoning applies to frequency division by N. Figure 7, Figure 8 and Figure 9 are the spectra of the FM signal after division by 6, 8 and 12 respectively. It is seen from Figure 9 that after division by 12, the resulting modulation index is less than 1 since there are only two significant side frequencies (narrowband angle modulation) separated by 1 kHz from a strong carrier component of frequency = $455 \text{ kHz} / 12 = 37.92 \text{ kHz}$.

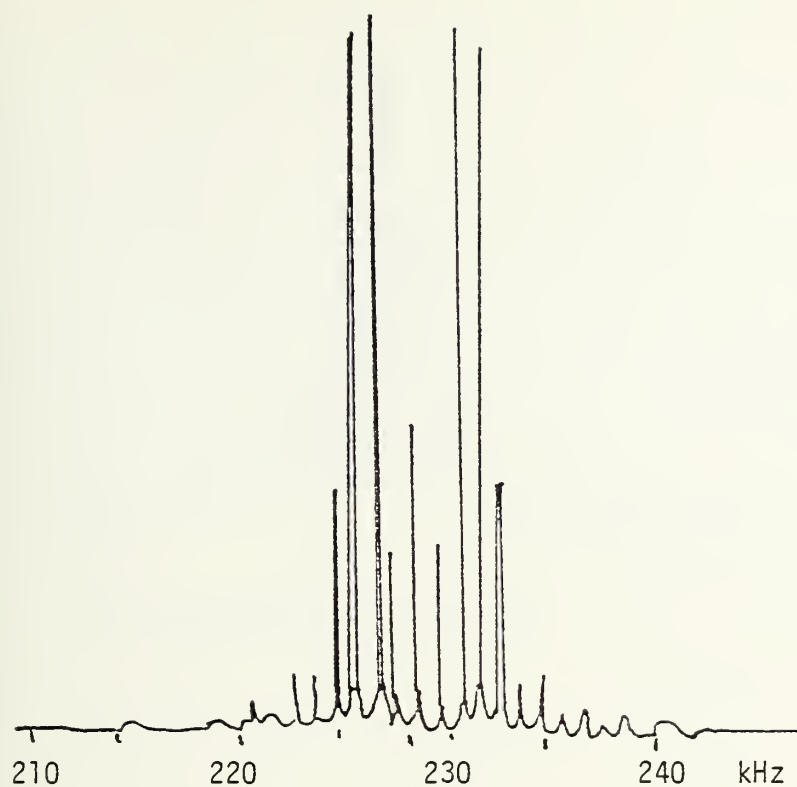


(a) Signal only (no noise).

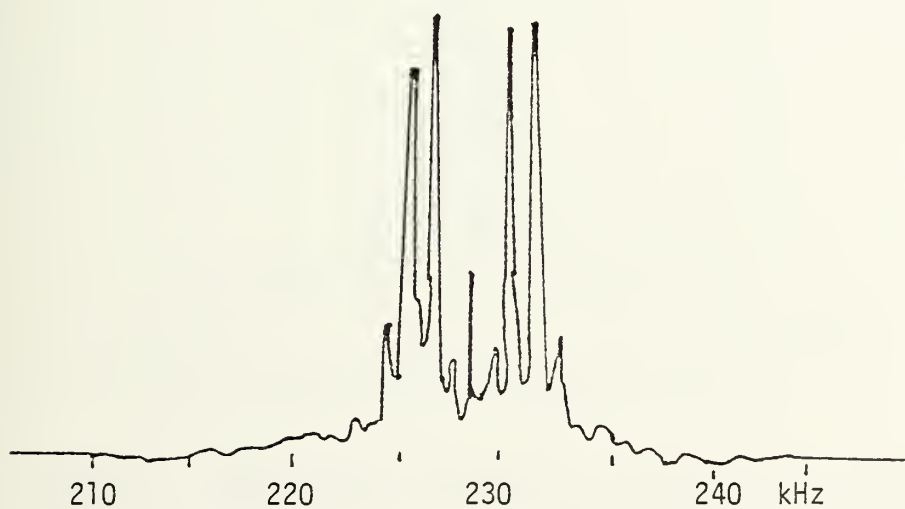


(b) Signal plus noise (SNR = 9.8 db).

FIGURE 5. SPECTRUM OF FM SIGNAL AT THE OUTPUT OF
HARD LIMITER ($f_c = 455$ kHz)

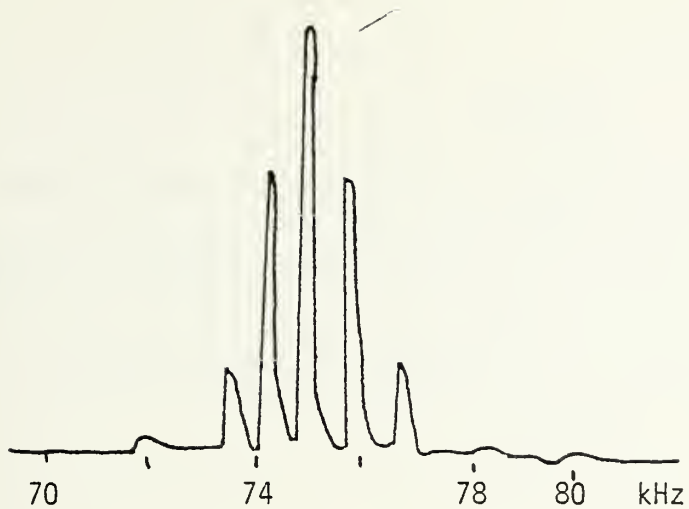


(a) Signal only (no noise).

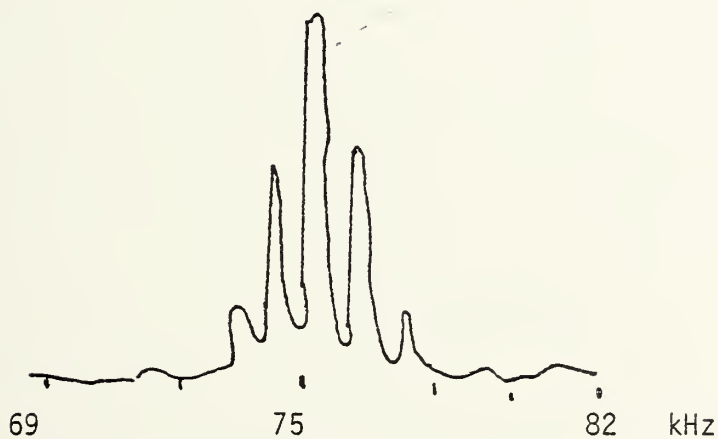


(b) Signal plus noise (SNR = 8.4 db).

FIGURE 6. SPECTRUM OF FM SIGNAL AT OUTPUT OF THE FREQUENCY DIVIDER, $N = 2$



(a) Signal only (no noise)



(b) Signal plus noise (SNR = 8.7 db).

FIGURE 7. SPECTRUM OF FM SIGNAL AT THE OUTPUT OF FREQUENCY DIVIDER, $N = 6$

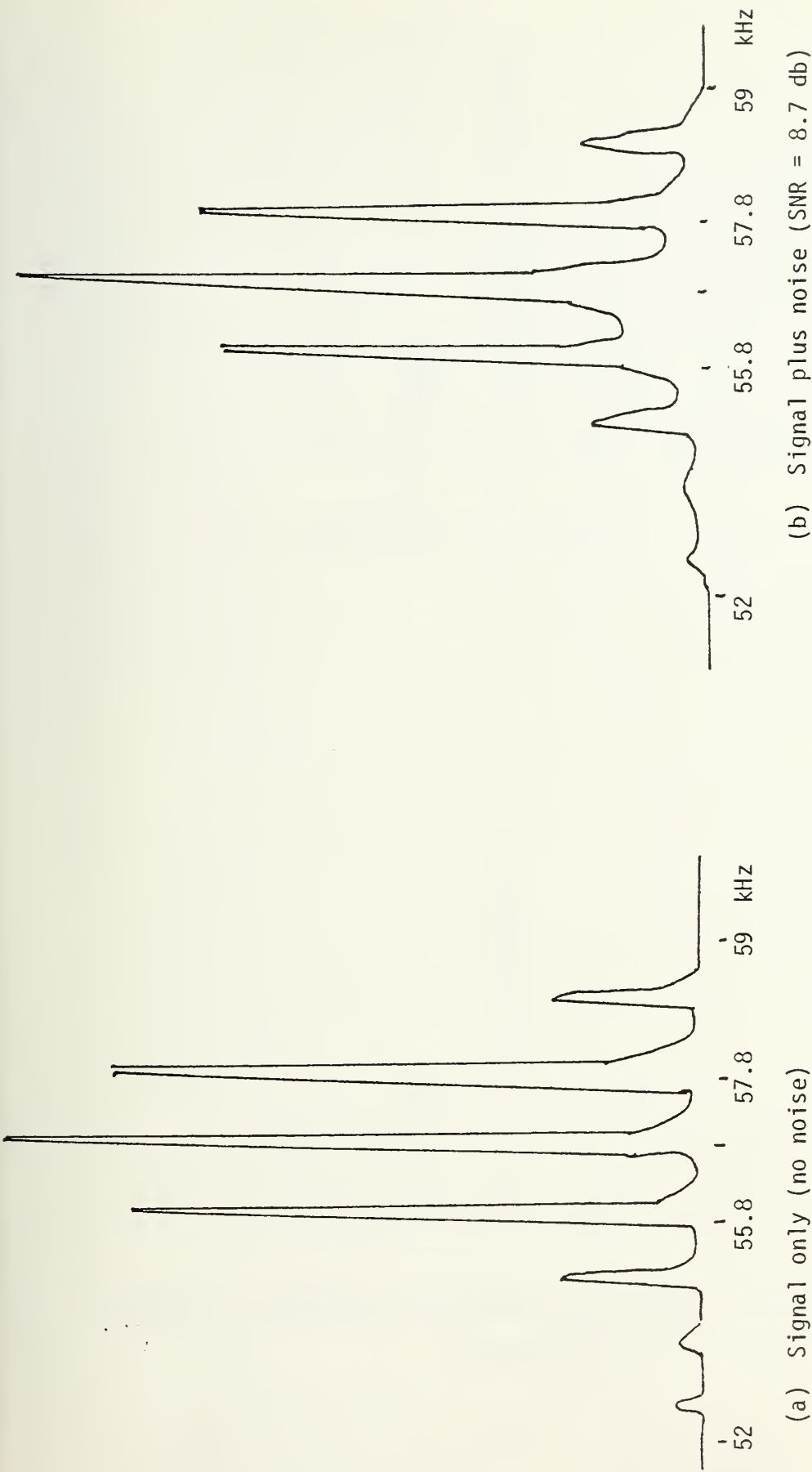
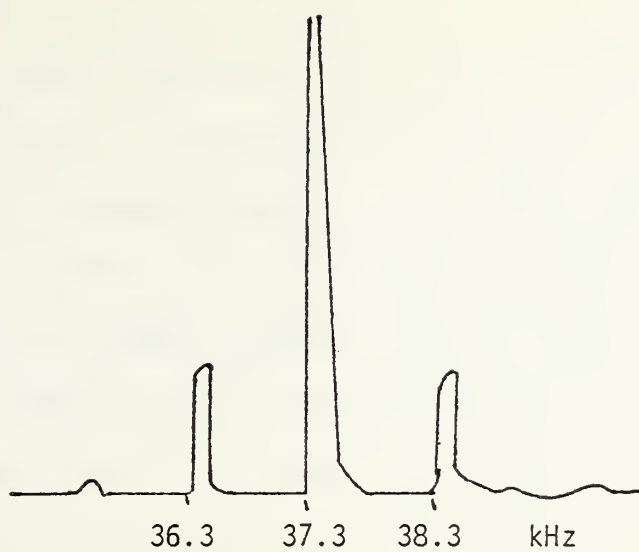
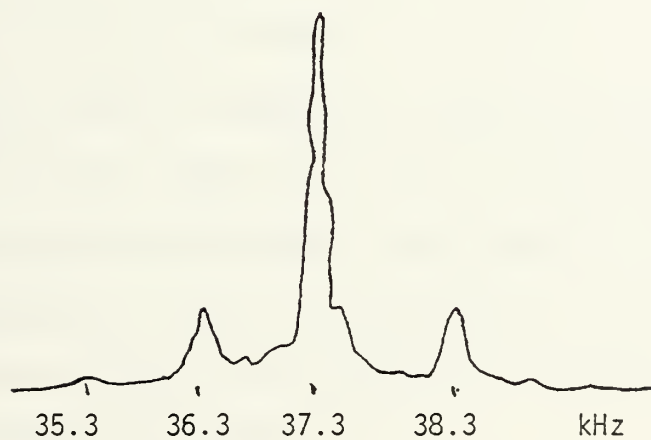


FIGURE 8. SPECTRUM OF FM SIGNAL AT THE OUTPUT OF FREQUENCY DIVIDER, $N = 8$



(a) Signal only (no noise).



(b) Signal plus noise (SNR = 7.9 db).

FIGURE 9. SPECTRUM OF FM SIGNAL AT THE OUTPUT OF FREQUENCY DIVIDER, $N = 12$

Of interest in this study is the plot of probability of error in the recovered data vs SNR at the input of the demodulator (hard limiter) portion of a receiver. These results are obtained by setting the data rate to 1 kHz and data amplitude to a level which provides a frequency deviation of the carrier such that all the significant sidebands of the FM carrier are in the same passband as that of the noise filtered by the mechanical filter. With no noise present the carrier level of the input to the hard limiter of Figure 2 is measured with the true RMS reading voltmeter. This reading when squared is a measure of signal power S . Noise is then added and the voltmeter read again. This reading when squared gives P which is a measure of signal power S plus noise power N_p (providing signal and noise are uncorrelated). SNR is formed as:

$$\frac{S}{P-S} = \frac{S}{N_p}$$

which becomes $10 \log \frac{S}{N_p}$ in decibels.

Probability of error is measured by using two digital counters. One counter records the number n_e of errors at the output of the error detecting circuitry described in the Appendix. Another counter records the number n_b of data bits transmitted in the time interval of interest. If the counters are activated for the same interval of time, then the probability P_e of error is:

$$P_e = \frac{n_e}{n_b} .$$

The pertinent results of this study are shown in Figure 1 which is a plot of probability of error P_e versus SNR in decibels for division by $N = 1, 2, 6, 8$ and 12 . The theoretical curve for non-coherent demodulation of a frequency-shift keyed (FSK) carrier is also shown [Ref. 2].

The results shown in Figure 1 indicate no significant change in system performance can be expected from frequency division. There is a reduction in signal bandwidth with frequency division as shown in Fig. 5 through Fig. 9. The receiving system noise can be reduced, therefore, by frequency division. However, the frequency deviation Δf of the carrier signal is also reduced (by a factor $\frac{1}{N}$). And with the PCD, the amplitude of the output signal $\hat{d}(t)$ (recovered data) is directly proportional to Δf . Thus, division by N reduces output signal level as well as input noise level. The result is no net improvement in system performance. It is expected that for values of SNR less than about 6 db the small signal suppression or capture effect of the hard limiter and frequency divider will result in the same deterioration in performance as experienced with other popular FM demodulators.

Early in this work, system operation and frequency division were tested using an analog signal consisting of music and human voice. The quality was judged by listening to the recovered signal. Results are that for $N = 1, 2, \dots, 8$, the output is practically noise free for SNR > 12 db. For $N > 10$ the same quality exists for SNR > 11 db. In all cases, the output is unusable when SNR < 4 db.

APPENDIX A

This Appendix is a description of the instrumentation and circuitry of Figure 2 in Section III of this report. The operation of each block is described here.

The square wave generator of Figure 2 is an Interstate Electronic Corporation (IEC) F35 AM/FM Function Generator. The output is a square wave of frequency twice that of the data rate of f_m Hertz. This data rate is divided by 2 by the error measurement gating circuit to form $d(t)$. This circuit also integrates the data of rate $2f_m$ Hertz to form a triangular waveform which is used to trigger the pulse generator. Figure A-1 shows the error measurement gating circuit.

Another IEC F35 AM/FM Function Generator is used as a frequency modulator to form $v_c(t)$. This instrument has a linear frequency vs voltage modulator characteristic in the frequency range used in this experiment.

The noise generator is a General Radio Model GR 1390B.

The mechanical filter is a Clevite ceramic filter TL 1009-20A having the passband characteristic shown in Figure 4(a).

The summing amplifier adds $n(t)$ to $v_c(t)$. The circuit uses an operational amplifier CA 3010 with appropriate compensation (connect a 1.3 kilohm resistor and a 39 picofarad capacitor in series between pins 11 and 12 and also between pins 6 and 7 as shown in Figure A-2.)

The hard limiter removes the amplitude variations of the signal $v_s(t)$ while preserving its frequency variation. Two transistors 2N3034 are used as voltage amplifiers to produce a sufficiently strong output to trigger the frequency divider (monostable multivibrator). To

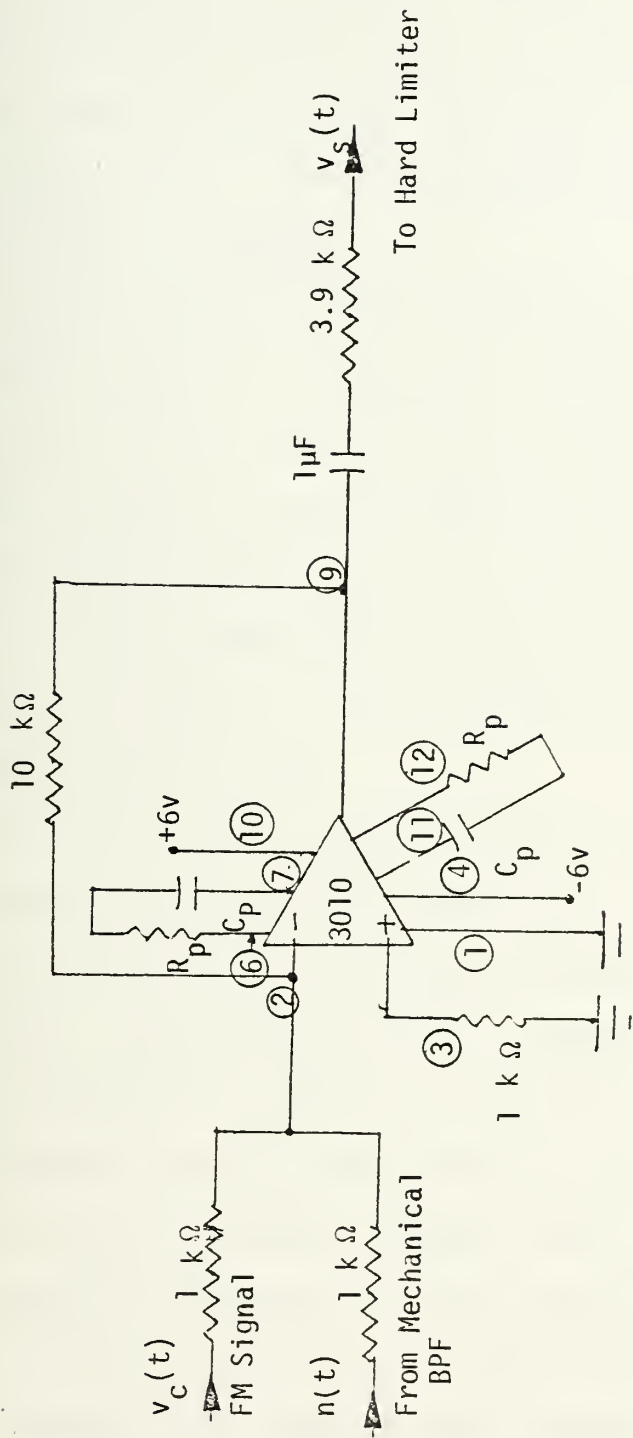


FIGURE A-2. SUMMING AMPLIFIER

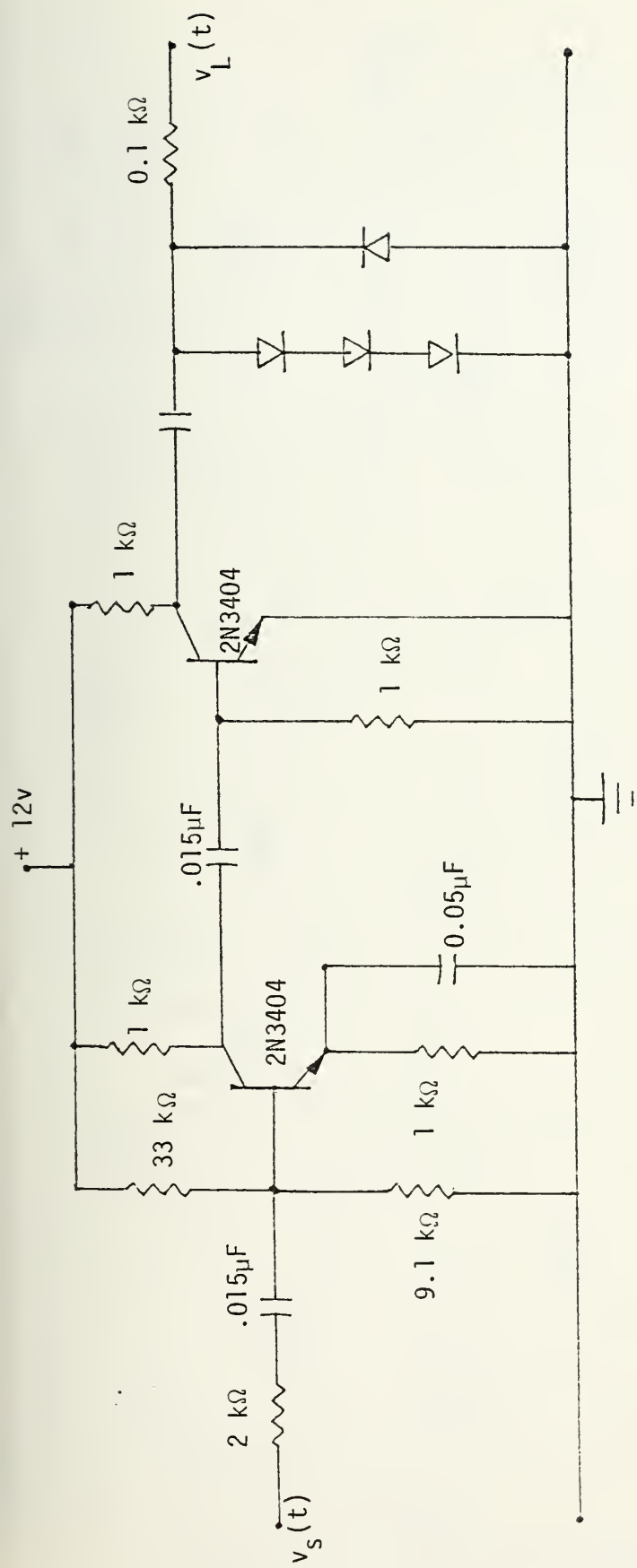
obtain a constant amplitude output $v_L(t)$, four switching diodes are used as shown in Figure A-3. These provide a peak-to-peak output voltage of approximately 3 volts which is needed to trigger the $\div N$ circuit.

The frequency divider reduces the transitions per second of $v_L(t)$ by the factor $\frac{1}{N}$ to form $v_N(t)$. The system built provides values of $N = 2, 4, 6, 8, 10, 12$. Figure A-4 shows the connections of the integrated circuits used as dividers.

The pulse counting demodulator (PCD) converts instantaneous frequency of $v_N(t)$ to voltage $v_d(t)$. The PCD consists of a monostable multivibrator and a lowpass filter (audio amplifier). A Schmitt trigger circuit is used to trigger the monostable multivibrator which generates one pulse each period of $v_N(t)$. The width of the pulse is variable from 30 ns to 40 μ s by changing resistor R_T and capacitor C_T in Figure A-5. A minimum pulse width of 30 nsec provides operation to a maximum carrier frequency of about 10 MHz.

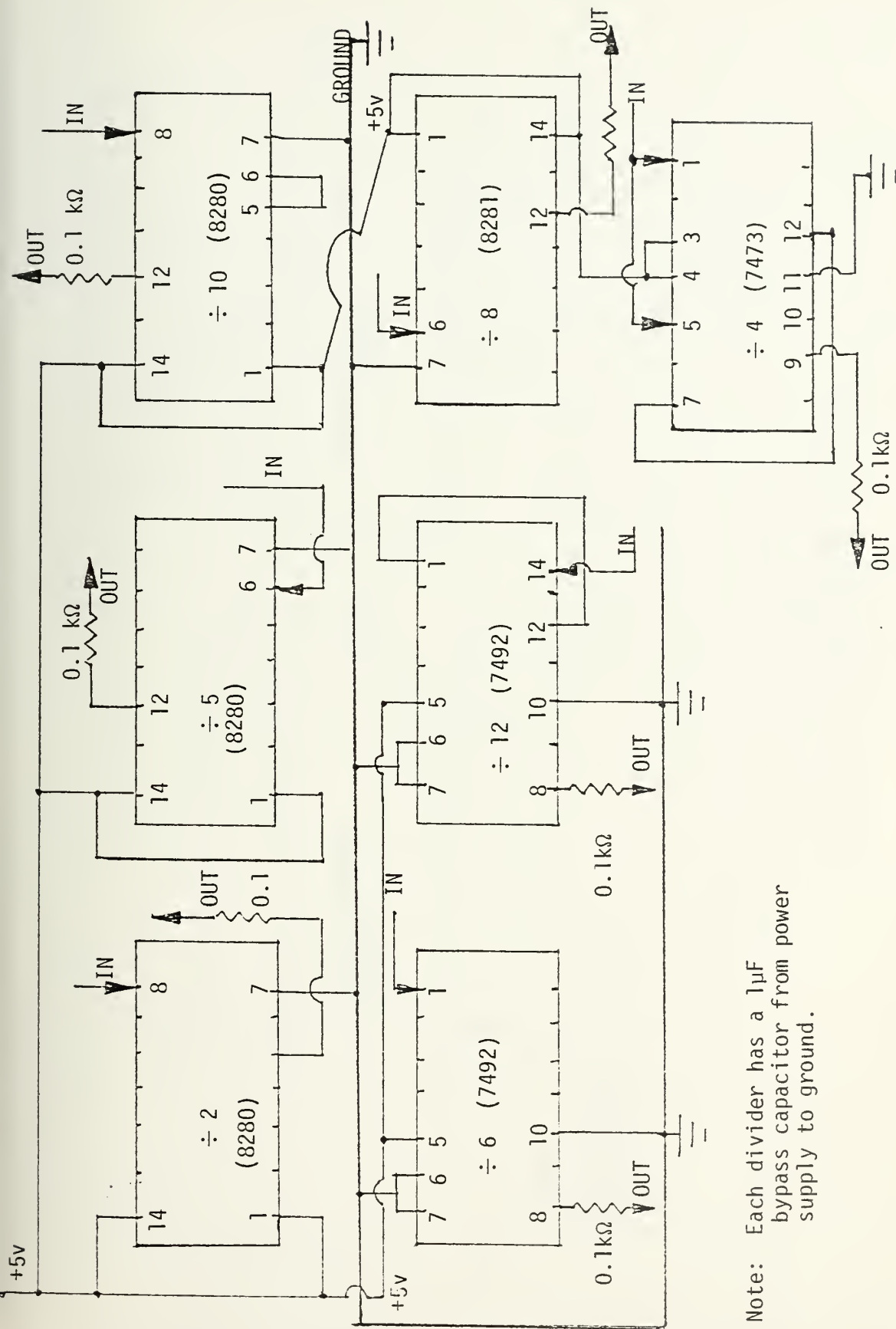
The low pass filter and audio amplifier averages and amplifies $v_d(t)$ to recover a replica $\hat{d}(t)$ of the data $d(t)$. The lowpass filter is a Krohn-Hite Model 3321 having measured frequency response shown in Figure A-6. The audio amplifier is a Hewlett-Packard Model 465A having an approximately flat frequency response from 0 to 200 kHz.

The error detection circuit consists of an integrator, amplifier, inverter, and two threshold circuits shown in Figure A-7. This circuit determines the presence of "1" bits or "0" bits when the recovered signal $\hat{d}(t)$ is applied. The recovered waveform $\hat{d}(t)$ is amplified and applied to a threshold circuit where a check is made for the presence of a "1" bit. Simultaneously, after integration, $\hat{d}(t)$ is inverted and also applied to another threshold circuit where a check is made for the



Notes: All diodes are silicon,
switching type.

FIGURE A-3. HARD LIMITER



Note: Each divider has a $1\mu\text{F}$ bypass capacitor from power supply to ground.

FIGURE A-4. CIRCUIT OF FREQUENCY DIVIDERS FOR

$N = 2, 4, 5, 6, 8, 10, 12$

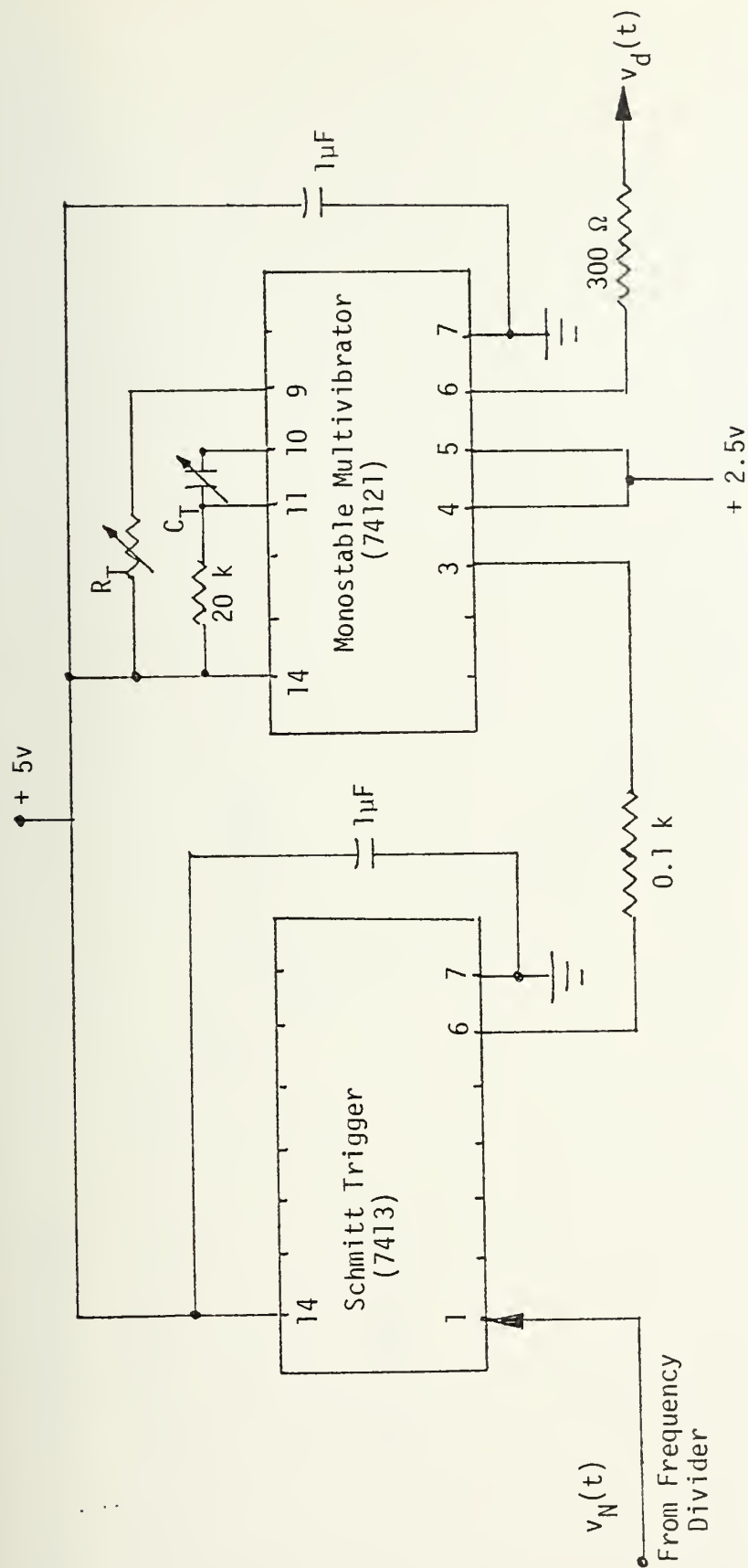


FIGURE A-5. PULSE COUNTING DEMODULATOR

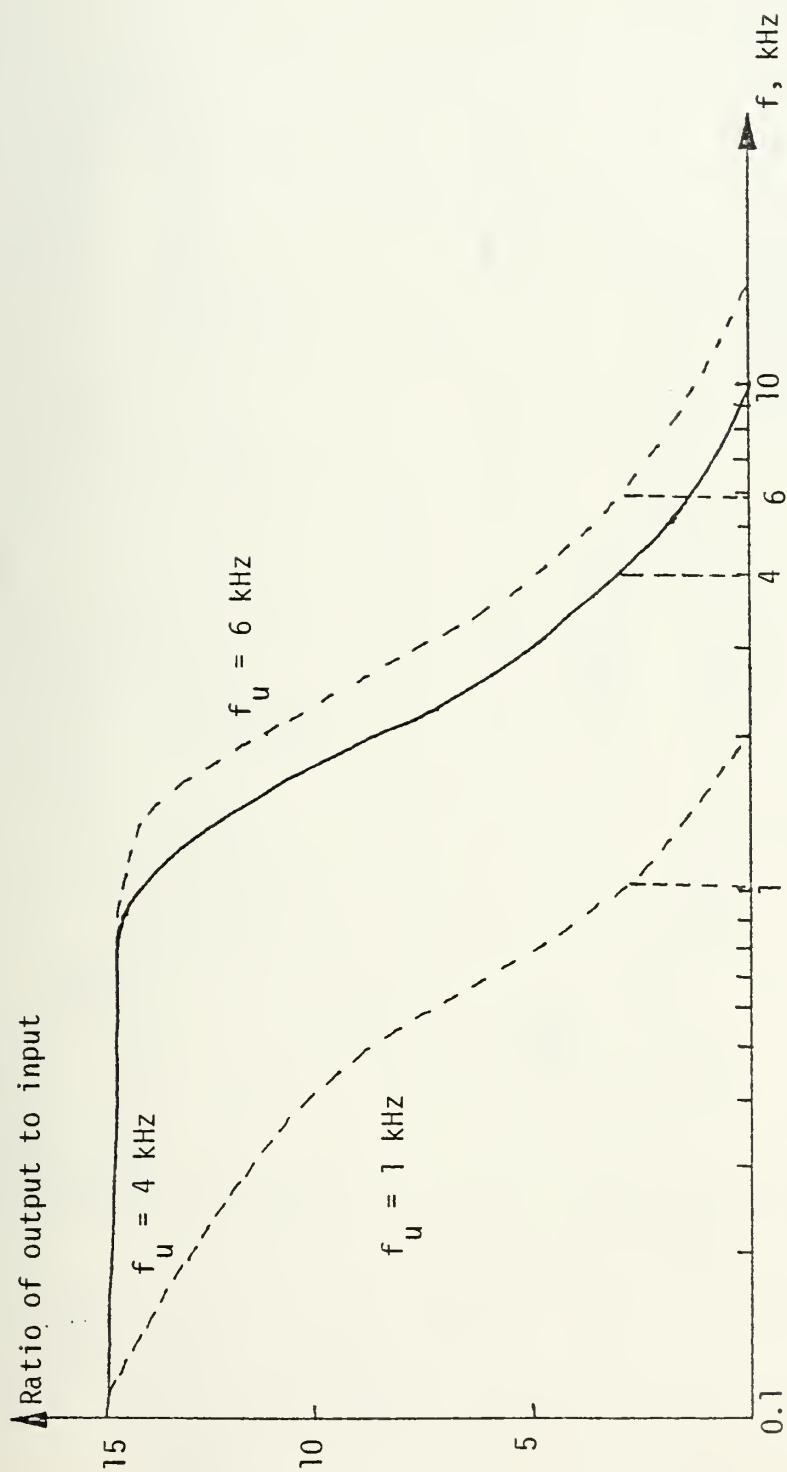


FIGURE A-6. FREQUENCY RESPONSE OF LOWPASS
FILTER WHEN CUT-OFF FREQUENCY
 f_u is 1, 4, and 6 kHz

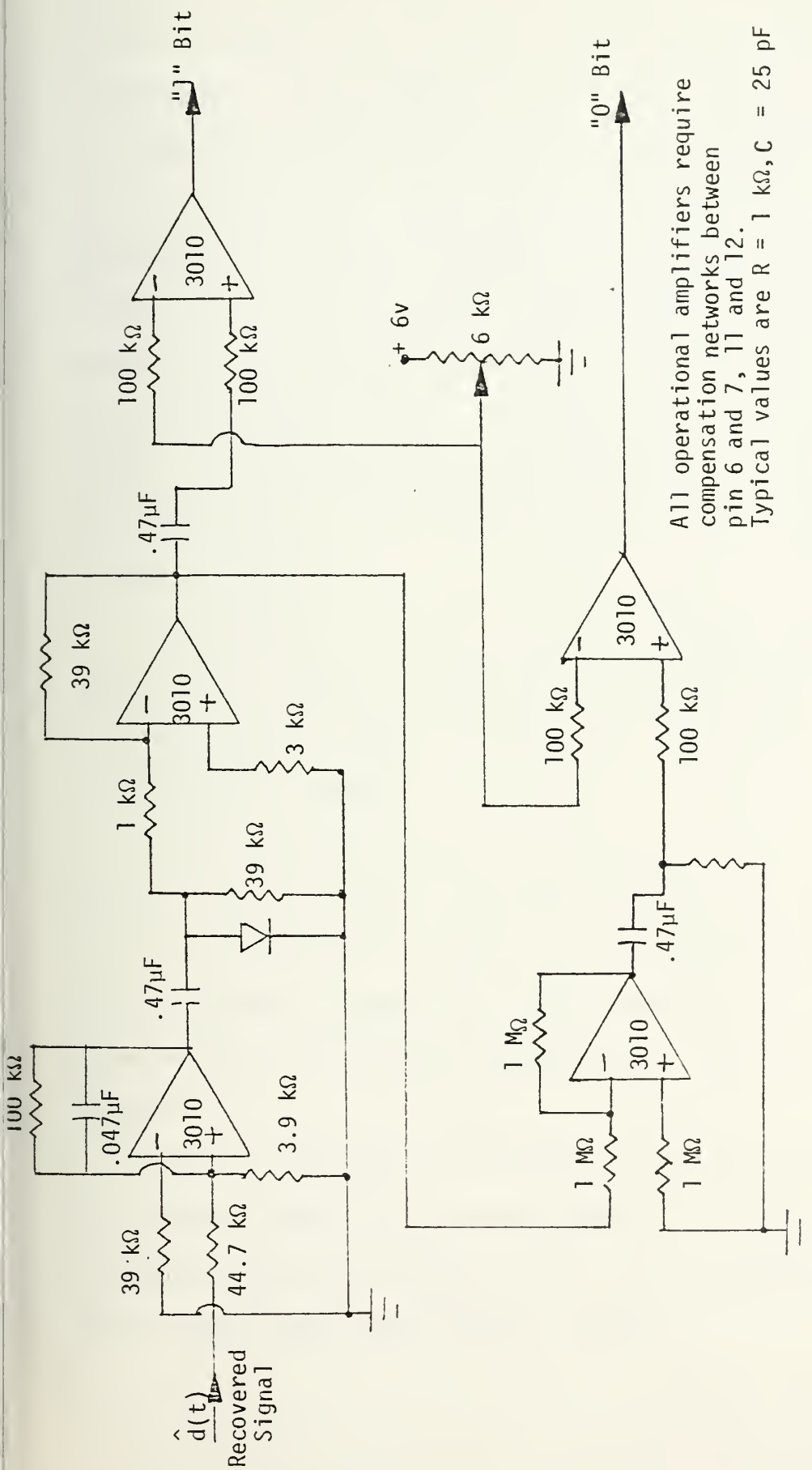


FIGURE A-7. ERROR DETECTION CIRCUIT.

presence of a "0" bit. Thus, the circuit has two outputs; one represents the presence of "1" bits while the other represents the presence of "0" bits. The two waveforms are identical except inverted.

The error decision circuit shown in Figure A-8 compares the "1" and "0" bit waveforms with input data $d(t)$. First, the "1" and "0" bit waveform are combined in an OR gate. The resultant waveform is identical to $d(t)$ with no error. This OR gate output and $d(t)$ are applied to an exclusive OR gate which compares the inputs and generates an output whenever a pulse $p(t)$ from the pulse generator occurs. This clocked output of the exclusive OR gate is a "1" whenever the inputs to the exclusive OR gate are dissimilar. This "1" is counted as an error.

The NAND gates in Figure A-8 are used as gates, inverters and delay lines as shown. The NAND delays and one OR gate are used merely to ensure $p(t)$ experiences the same delay through the circuit as the "1" and "0" bit signals.

The pulse generator is a Data Pulse Model 101 which is triggered by the triangular wave $v_T(t)$. Since the frequency of $v_T(t)$ is twice that of $d(t)$, the pulse $p(t)$ is made to occur near the middle of each bit of $d(t)$ as shown in Figure A-9. Thus, a decision concerning the error between $d(t)$ and $\hat{d}(t)$ is made midway between transitions of these waveforms.

The data counter counts the number of bits in an interval of time (10 seconds, typically). The error counter counts the number of error detected in that same interval of time. Both instruments are Hewlett-Packard Model 5302A general digital counters.

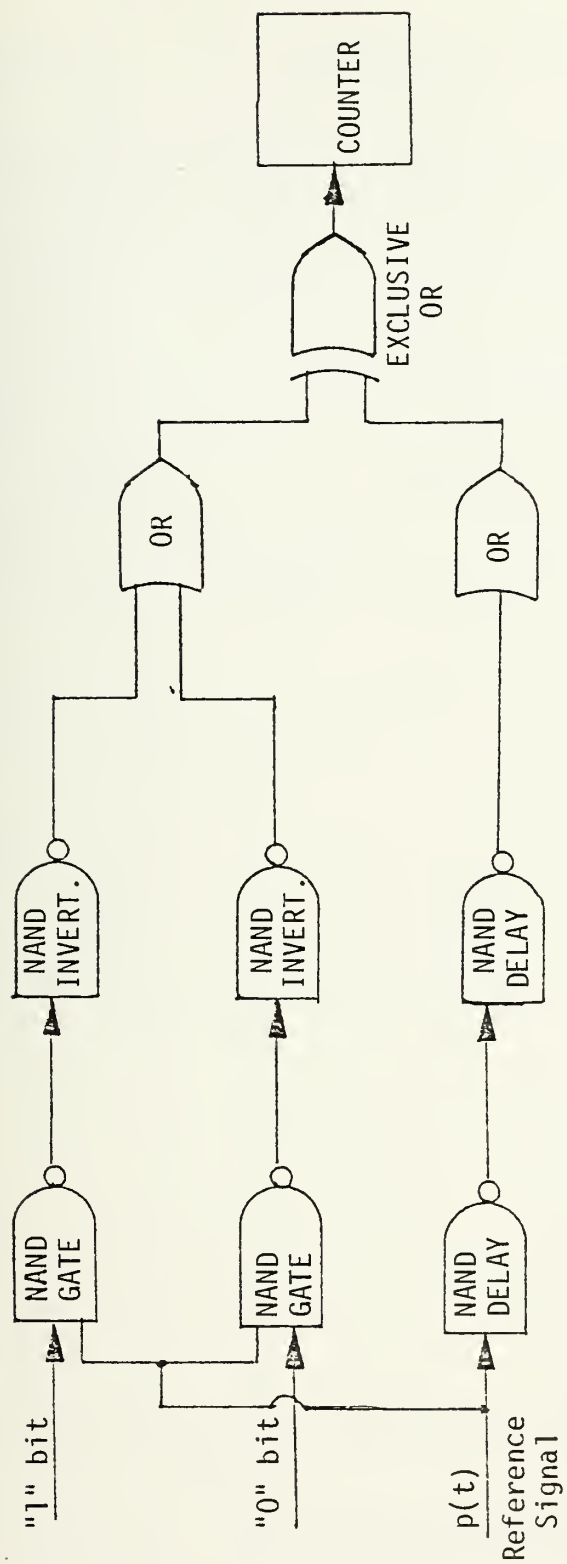


FIGURE A-8. ERROR DECISION CIRCUIT

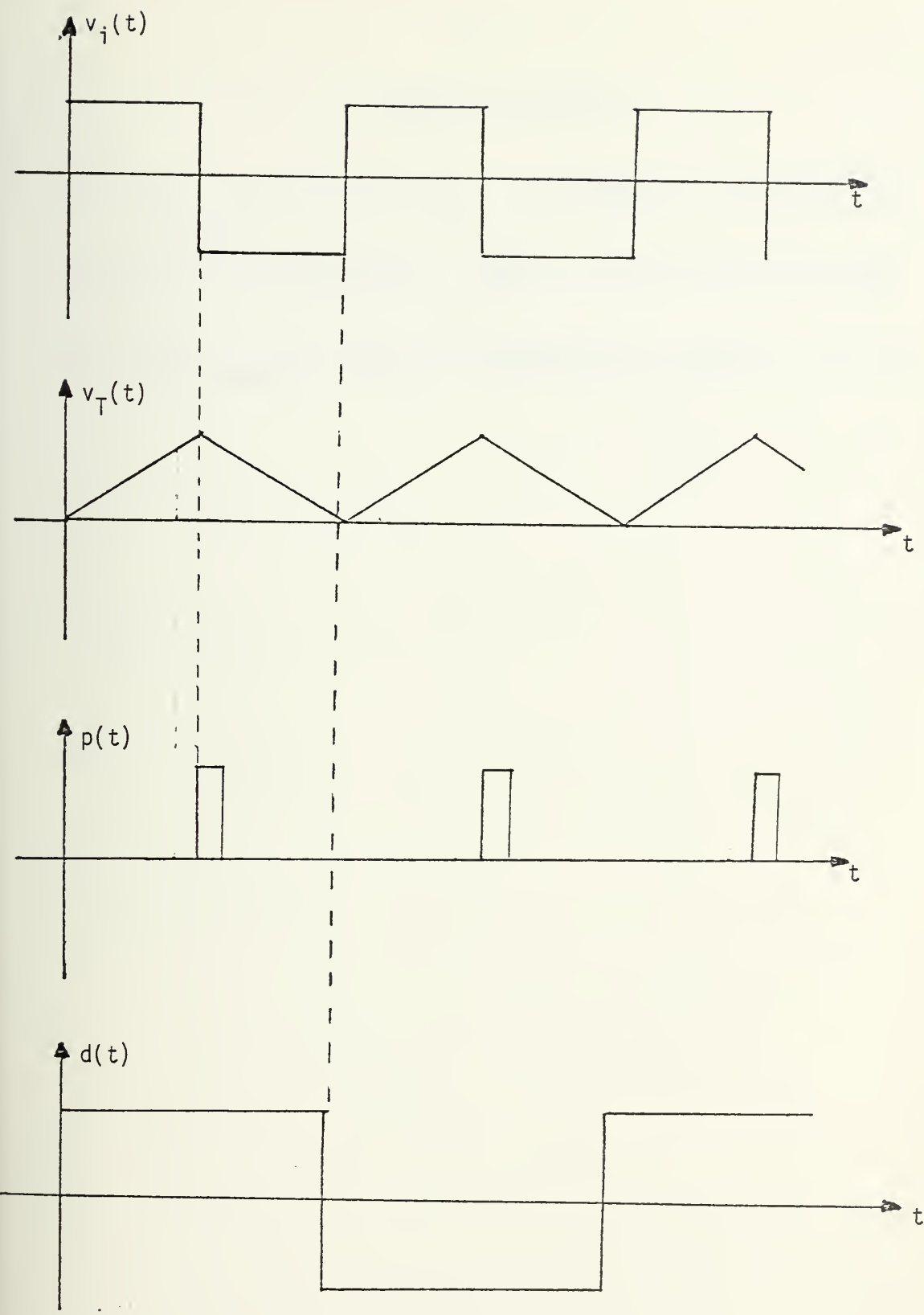


FIGURE A-9. WAVEFORMS ASSOCIATED WITH ERROR CIRCUITS

LIST OF REFERENCES

- [1] Taub, H. and Schilling, D. J., Principles of Communication Systems, p. 117-127, McGraw-Hill, 1971.
- [2] Stein, S., and Jones, J.J., Modern Communication Principles, p. 236-241, McGraw-Hill, 1967.
- [3] Clark, K.K. and Hess, D.T., Communication Circuits: Analysis and Design, p. 571-625, Addison-Wesley, 1971.

INITIALLY DISTRIBUTED REPORT

INITIAL DISTRIBUTION LIST

	No. Copies
1. Library, Code 0142 Naval Postgraduate School Monterey, California 93940	2
2. Department Chairman, Code 62 Department of Electrical Engineering Naval Postgraduate School Monterey, California 93940	2
3. Assoc. Professor Glen A. Myers, Code 62Mv (thesis advisor) Department of Electrical Engineering Naval Postgraduate School Monterey, California 93940	2
4. Assoc. Professor Rudolf Panholzer, Code 62Pz Department of Electrical Engineering Naval Postgraduate School Monterey, California 93940	1
5. Professor George A. Rahe, Code 62Ra Department of Electrical Engineering Naval Postgraduate School Monterey, California 93940	1
6. Mr. Duong tuan Viet 1164 Third Street Monterey, California 93940	1

Thesis
V663 Viet
c.1

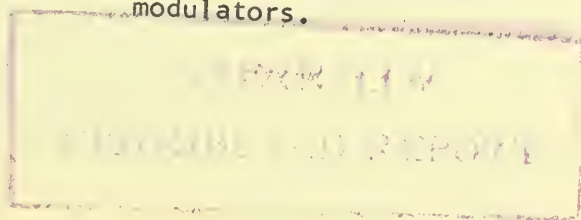
166621

Measured effects of
frequency division on
the performance of pulse
counting frequency de-
modulators.

Thesis
V663 Viet
c.1

166621

Measured effects of
frequency division on
the performance of pulse
counting frequency de-
modulators.



thesV663

Measured effects of frequency division o



3 2768 000 99401 6

DUDLEY KNOX LIBRARY